Preparation and Characterization of Layered Silicate Polyethylene Terephthalate Nanocomposite by in Situ Polymerization

Ali Esmailzadeh*, Fatemeh Rekabdar, Ali Mehdizadeh, and Ghasem Khatinzadeh

Technology Development of Chemical, Polymeric, and Petrochemical Research Division, Research Institute of Petroleum Industry (RIPI), Tehran, Iran

ABSTRACT

A series of experiments on the synthesis of poly (ethylene terephthalate) (PET)/organo-montmorillonite (MMT) nanocomposites were carried out in a pressurized reactor using alkyl ammonium exchanged smectite clays, (Closite 30B). Given the degradation of organoclay at high temperatures, the in situ polymerization process was carried out at mild temperatures ranging from 210 to 230°C for 40 minutes followed by solid state polymerization (SSP) at 245°C for 30 minutes at a pressure of 5 mbar. The nanocomposites were prepared using different weight percentages (1-5) of organoclay. The reaction completed when the mixing torque ceased to change as recorded by the auto data acquisition system of the pressure reactor. The DSC analysis provided information on the course of the thermal characterization of the PET nanocomposites versus regular PET. As shown by the results of DSC cooling scan, all the PET nanocomposite samples have higher crystallization temperatures (T_c) and faster crystallization rates ($\Delta H_C/t$) compared to regular PET. Furthermore, the opposite behavior is observed for $t_{1/2}$. This is due to the fact that the nucleation of organoclay nanoparticles reduces the crystallite size in the PET nanocomposites. The XRD results indicated that the peaks in the 2θ angle from 1° to 7° were disappeared, which is an indication of an exfoliated MMT. In addition, The atomic force microscope (AFM) results showed broken mirror like lamellae, confirming the exfoliated results of the XRD analysis. The peaks are indexed according to the 2θ angle from 10° to 30° known assignments of the triclinic unit cell dimensions for PET. The comparative crystallite size of the PET nanocomposites samples (1-5%wt organoclay) can be deduced from the peak ratio change of 2θ angle from 10° to 30°. Heat distortion (or deflection) temperature (HDT) was enhanced by increasing the amount of organoclay in PET nanocomposites compared to regular PET. The tensile test results of 2%wt organoclay show an increase of 58% in the tensile strength of this sample. As a result of MMT agglomeration, due to the high temperature instability of Closite 30B, the relative oxygen pressure drop data shows fluctuations. However, as an overall trend, PET nanocomposite gives about 50% greater reduction in O_2 pressure drop or relative oxygen permeability compared with a homo structure.

Keywords: Poly (Ethylene Terephthalate), Montmorillonite, Nanocomposite, Exfoliated, In situ Polymerization.

***Corresponding author**

Ali Esmailzadeh*

Email: esmailzadea@ripi.ir

Tel: +98 21 4825 2446

Fax: +98 21 44739517

Article history

Received: May 14, 2014

Received in revised form: November 11, 2014

Accepted: January 01, 2015

Available online: October 20, 2016

INTRODUCTION

Incorporating organo MMT aggregates to form nanocomposites is a very important method to significantly improve certain polymer properties. The final properties of the nanocomposites are affected by their morphology [1]. In general, by increasing the aspect ratio of the MMT, the interfacial bonding and the polymer matrix reinforcement are improved [2].

Annually, 800,000 tons of poly (ethylene terephthalate) are produced in Iran. An extensive research interest has lately evoked the preparation of various novel polymer-organo-Montmorillonite (MMT) nano-composite materials with advanced physical, thermal, and mechanical properties. The layered silicate can act as a nucleation agent [3, 4]. PET nanocomposite prepared by in situ poly-merization using organoclay (Closite 30B) produces materials of advanced gas barrier properties [5], thermal stability [6], and mechanical strength [7,8]. Although in situ technique presents a high potential route for the dispersion of the layered silicate in the polymer matrices at nano meter scale, it suffers from some drawbacks [9].

Direct condensation reactions of diol and diacid functional groups in the presence of clay result in the generation of low molecular weight polymers, whereas the synthesis of the nanocomposites by melt intercalation approach only gives a small extent of polymer intercalation in the interlayer of organoclay. Due to the better dispersion of the layered silicate in the polymer matrices and thus more interaction between Closite 30B functional groups with PET, the in situ technique accompanied with solid state polymerization (SSP) was developed. The combination methods of solution intercalation [11] and melt polymerization process [12-15] of PET nanocomposites were studied in our previous work [10]. The novelty of the this work is that the layered silicate has been added to the polymer matrices after the octamer formed via in situ polymerization in order to solvate a small extent of polymer intercalation. Although melt polymerization can increase molecular weight higher than viscosity value (0.80 dL/gr), this process can cause resin quality problems due to the degradation caused by high temperatures and long reaction times. Such melt polymerization is performed at moderate temperature and short residence time. SSP is then carried out for reaction completion under relatively moderate thermal conditions. The important roles of SSP are increasing the molecular weight with less thermal degradation than melt phase polymerization and to reduce the contents of by-products such as acetaldehyde and oligomers. The normal SSP temperature is 200 ~ 230°C [16]. Apart from this study, PET nanocomposites were investigated by combined DSC, XRD, and AFM measurements to characterize the morphology and properties of those products. In this work, triclinic crystalline size decreases as a result of organo–MMT addition followed by the XRD and AFM for the first time.

EXPERIMENTAL PROCEDURES

Materials

PET oligomers (with DP=12 and η_{int} =0.24 Intrinsic Viscosity deciliter/gram), bis(2-hydroxylethyl) terephthalate, antimony trioxide and acetate as catalysts, cobalt acetate as a colorant, antifoam, metal stabilizer and antioxidant were received from Shahid Tondgooyan Petrochemical Company (Iran). Organo-modified montmorillonite Closite 30B was supplied by Southern Clay Co, USA. The chemical structure of the organomodifier is shown in Figure 1.

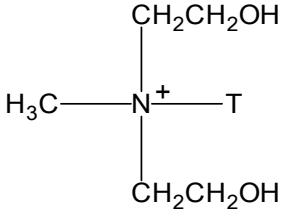

Figure 1: Chemical structure of organomodifier used in Closite 30B. *T* is tallow (65% C_{18}; 30% C_{16}; 5% C_{14}).

In Situ Polymerization of PET/Organo-MMT Nanocomposites

Synthesis of organoclay MMT/PET nanocomposite using Closite 30B was performed in a Buchi pressure reactor shown in Figure 2. The SSP process of PET nanocomposite included two stages, namely drying at 170°C for one hour and stepwise polycondensation process at temperatures of 210-230°C for 40 minutes. Subsequently, the reaction mixture was ground to pills of about 0.3 mm particle size and then the SSP of chips was carried out at 245°C for 30 minutes at a pressure of 5 mbar. The reaction was carried out at different organoclay weight percentages (2, 3, 4, and 5) and the product was characterized using XRD, AFM, and DSC.

The viscosity of PET nanocomposite samples and subsequently the reaction times were controlled by monitoring the torque used for the stirring of Buchi reactor.

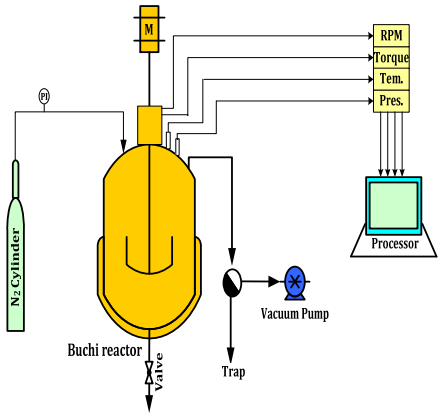

Figure 2: Schematic drawing of nano PET in situ polymerization reactor.

XRD Analysis

The basal spacing of the nanocomposites and clays were determined by a wide angle X-ray diffraction technique (XRD); (Philips PW 1840, Cu, K-α radiation: 1.541 Å). The analyses were meant to measure the *d*-spacing of organoclay and the nanocomposites with 1-5 %wt organoclay at a scanning rate of 0.02°/sec in the range of 2θ=1°-30° at 45 kV and 40 mA.

AFM Measurements

Atomic force microscopy (AFM) is a type of scanning probe microscopy showing the topography of a polymer surface. This technique provides the resolutions in angstrom range. The atomic force microscope consists of a very fine tipped probe, which is positioned several angstroms above the surface of the polymer material. The tunneling current between the tip of the probe and the surface is then measured. The silicon nitride probe is attached to a cantilever with a reflective surface. A piezo-electric support is applied in order to mount the sample and move in response to surface changes sensed by the probe. The resulting deflections are monitored by the reflected laser beam [17]. Measurements can be made in contact and rapping modes, with and without the oscillation of the cantilever respectively.

Relative Oxygen Permeability

The relative oxygen permeability tests of PET nano composite films with different clay %wt loadings were performed using the cell permeability test depicted in Figure 3. These tests were carried out at a temperature of about 23°C and a pressure of 15 atm for 30 days. The films were cut to fit the 12 cm^2 area of the test holder of the permeation cell.

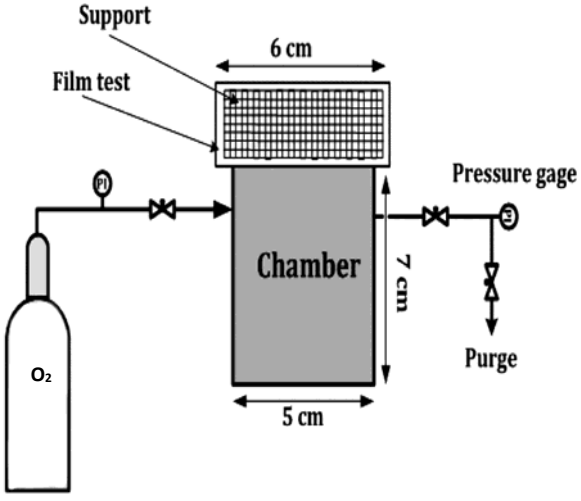

Figure 3: Schematic of the experimental set-up for measuring the relative oxygen permeability of the films.

DSC Analysis

A Perkin Elmer DSC-7 (Shelton, CT) differential scanning calorimeter was used to perform the thermal analysis and study the crystallization behavior of PET nanocomposites.

The effects of nanoparticles on crystallization behavior of PET polymer were studied through the proper weighing of samples (8-10 mg), dried at 110°C in vacuo overnight, introduced into the DSC, heated to 300°C, and then cooled to 40°C at a cooling rate of 10°C/min under a nitrogen atmosphere.

As the crystallization peak is symmetrical in nature, the half crystallization time ($t_{1/2}$) of non-isothermal cooling can be obtained using the following equation [18].

$$t_{1/2} = (T_{c,on} - T_c) / \chi$$

where $t_{1/2}$ represents the time required for the nanocomposites to reach 50% relative degree of crystallinity; $T_{c,on}$ is the crystallization onset temperature (temperature at which the thermograph initially departs from the baseline), and T_c is the temperature where the exotherm shows a peak; χ is the cooling rate (°C/min). This was used to evaluate the initial rate of PET nanocomposite crystallization. Since the layered silicate can act as a nucleating agent [3, 4], the $t_{½}$ values of the nanocomposites are smaller than those of pure PET [19].

RESULTS AND DISCUSSION

Polymerization

In situ polymerization process at 275°C for two hours reduces the nanocomposite quality as a result of the agglomerations shown in Figure 4. These agglomerations appear on the surface of reactor due to the production of degraded clay, coming from severe polymerization conditions. In order to reduce clay agglomeration in the nanocomposites, moderate reaction time and temperature should be applied.

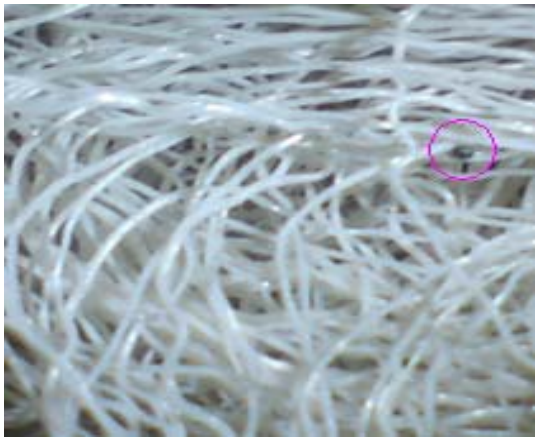

Figure 4: The stained product due to the degraded organomodified clay is shown inside the circle.

The thermal degradation of the nanocomposites can be followed by the stained product or IR spectroscopy via increasing the carboxyl and decreasing the hydroxyl end group concentrations at 3268 cm^{-1} and 3545 cm^{-1} respectively [20]. The product contamination, shown in Figure 4, was removed by the implementation of SSP under mild processing conditions.

Using SSP method, molecular weight can be increased with thermal degradation less than melt phase polymerization and an inherent viscosity increase from 0.59 to 0.70, as shown in Table 1. The SSP reaction temperature is normally about 220°C and can be increased up to 245°C according to melting point of the growing PET molecular length.

Table 1: Inherent viscosity (dL/g) of PET and Nano PET (ASTM D 4603– 96).

PET Octamer	PET Industrial chips (Shahid Tondgooyan Petrochemical Company)	PET nanocomposite (3% - Closite 30B)	
		Before SSP	After SSP
0.24	0.71	0.59	0.70

As the reaction proceeds, the reactants become more and more viscous. Consequently, more torque is required for a constant stirring rate. By monitoring the torque value, the reaction progress can be estimated [21] and so can the inherent viscosity of corresponding PET nanocomposite. The greater slope of the viscosity curve for pure PET indicates the initial rate of polymerization step for the pure PET, which is greater than that of the nanocomposite in Figure 5. The low permeability of the nanocomposite causes striping of the by-product and thus decreases the polycondensation rate. Recently, similar results have been published, which report that the decreasing rate of SSP reactions in the nanocomposites indicates that the organoclay platelets restricts the mobility of the reactive groups and increases the diffusion path length of the by-products [22].

The torque data and the viscosity, both of which depend on the growing PET molecular weight, agree well the data reported by M. Dini et al. [23].

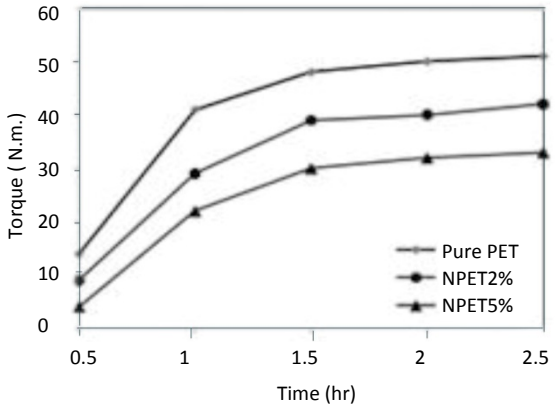

Figure 5: Dynamic viscosity growth represented as torque increases with reaction time.

Less viscosity value for the final nanocomposite product in comparison with pure PET may be due to organo-MMT acting as lubricant [24], reducing polymer entanglement and molten polymeric chains absorbed on MMT. This allows MMT layers of the nanocomposite to slide easily over each other. Chain alignment on MMT causes a reduction in entanglement. By increasing organo MMT sliding happens more easily and thus viscosity decreases as a result (Figure 6).

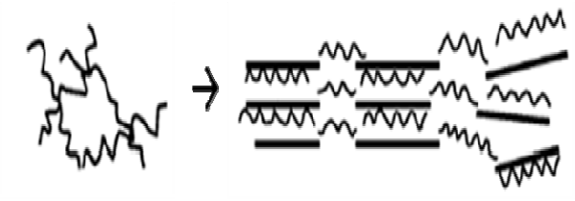

Figure 6: Molten polymeric chains alignment on MMT surface.

Poly (ethylene terephthalate) is relatively difficult to process compared to other thermoplastics. According to the addition of MMT loading, the ability of the molten nanocomposite to flow will also be improved [24]. In conclusion, MMT increases the processability of the nanocomposites.

Thermal Characterization

Differential scanning calorimetric (DSC) analysis provides information on the course of thermal characterization of the nano-PET versus regular PET samples. Table 2 shows the thermal analysis of cooling scan or non-isothermal results for all the samples.

Table 2: DSC cooling data for pure PET in comparison with NPET (nano-PET).

Sample	T_c (°C)	T_{on}(°C)	$t_{1/2}$ (min)	Crystallization rate[36] $\Delta H_c/t$ J/(gr/s)
Pure PET	159.38	178.17	1.879	0.1936
NPET 1%	185.20	191.67	0.647	0.4739
NPET 2%	182.68	195.50	1.282	0.3510
NPET 3%	172.97	189.93	1.692	0.2448
NPET 4%	189.06	194.50	0.544	0.4340
NPET 5%	187.97	200.17	1.210	0.3917

Half time of crystal formation ($t_{1/2}$)
Crystal formation temperature (T_c)
Onset crystal formation temperature (T_{on})

$t_{½} = (T_{on} - T_c)/ \chi$

χ is the cooling rate (°C/min) and $t_{1/2}$ shows the time to reach 50% of the relative degree of

crystallinity [18]. It is obvious that the rate of crystallization is strongly dependent on the temperature and the crystallization of the nano PET can be conducted faster at a higher cooling rate [25]. Crystallization process originates from the nucleation of crystallites [26].

As shown in Table 2, at the same cooling rate (10°C/min), all the nano PET samples have higher crystal formation temperature (T_c) and a higher rate of crystallization (ΔH_c/t) compared with the regular PET samples. In addition, the opposite behavior is observed for the half time of crystal formation ($t_{1/2}$). This phenomenon indicates the fact that nanoparticles behave as nucleating agents during crystallization, which can potentially reduce the crystalline size in the PET nanocomposites.

As observed in Figure 7, the crystallization peaks shift toward to the right and become sharper with increasing organoclay. Similar phenomena were also reported previously for a similar polyester/Cloisite30B system [27].

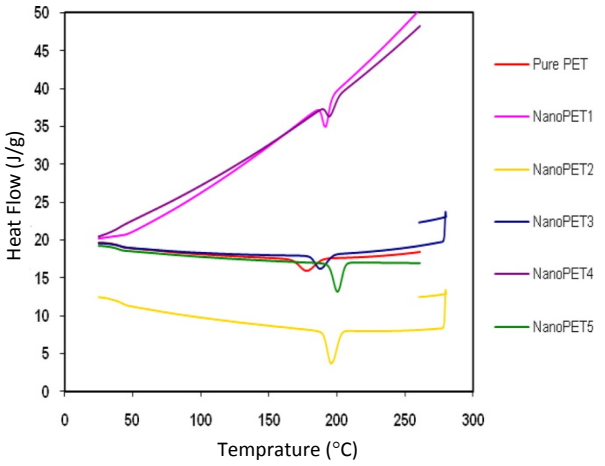

Figure 7: DSC thermograms of pure PET and PET nanocomposites (cooling scans).

Morphology and Properties

The XRD results showed the disappeared peaks in the 2θ angle from 1 to 7°, which is the indication of an exfoliated MMT (Figure 8). In addition, the image analysis of atomic force microscope confirms the exfoliated results of XRD analysis. The intensity of WAXS diffraction peak in the range of 2θ angle from 10 to 30° of triclinic unit cell planes indicates the size of PET crystal [22, 29]. The peak at 2θ = 17.8° corresponds to the (010) diffraction plane of the triclinic crystal of PET [29].

Increasing organo-MMT amount broadens XRD spectrum in the 2θ angle from 10 to 30° region, showing crystals are getting smaller (Figure 9).

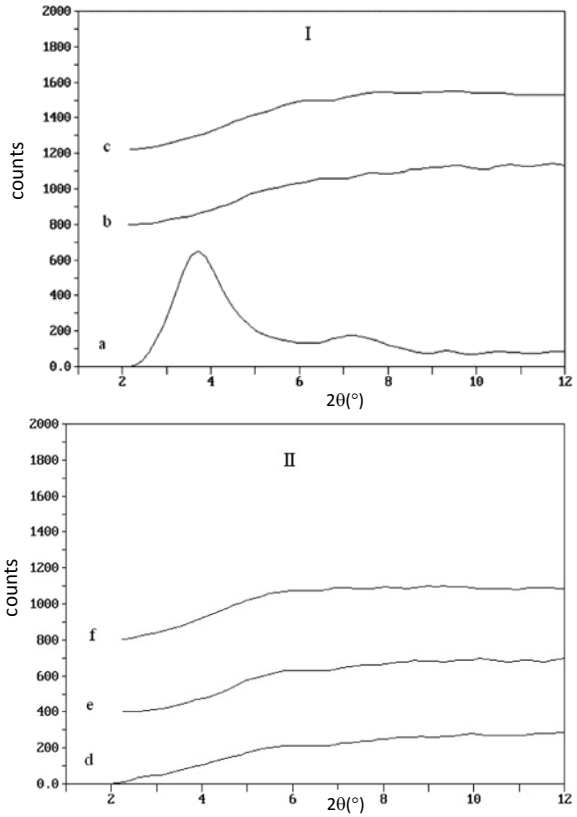

Figure 8: XRD patterns of organoclay and the nanocomposites: (a) organoclay; b (1%); c (2%); d (3%); e (4%); and f (5%) organoclay content.

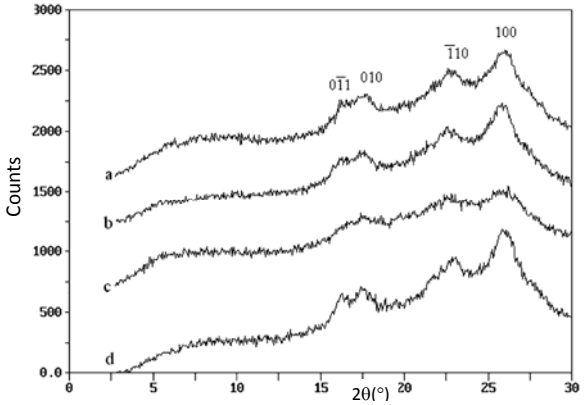

Figure 9: XRD patterns of the nanocomposites: (a) 3 %wt; (b) 4%wt; (c) 5%wt organoclay; and (d) pure PET.

The reduction of the crystal size as a result of increased MMT causes X-Ray scattering and therefore makes XRD spectra broader [30]. At an MMT concentration of 5 %wt, the smallest crystals are obtained with almost the disappearance of XRD spectra. The AFM studies and DSC measurements have led to the same results.

Mechanical properties were improved with increasing the weight percent of organoclay as shown in Table 3.

Thermal resistance (heat distortion temperature) of the nanocomposite was enhanced by increasing the weight percent of organoclay (Table 4).

Closite 30B materials possess two hydroxyl groups in their modifier (Figure 1), which enable them to interact with PET hydroxyl and carboxyl groups. This promotes the proper intercalation of PET molecules into clay gallery (Figure 10).

Table 3: Elongation, modulus, and tensile data of the classic and nano PET (ASTM D638)

Organoclay %wt loading	Tensile Strength (kg/cm^2)	Maximum load at break or breaking point (kg°F)	Elongation at break (%)	Tensile Modulus (N/mm^2)
(Pure PET)	310	23.2	7.5	385
PET-Organo. MMT 1 %wt	328	35	7	411
PET-Organo, MMT 2 %wt	531	41	10	492

Table 4: HDT data of the classic and PET nanocomposites with various amounts of MMT (ASTM D648)

(Pure PET)	PET-Organo MMT 1 %wt	PET-Organo MMT 2 %wt	PET-Organo MMT 3 %wt
68	71	74	83

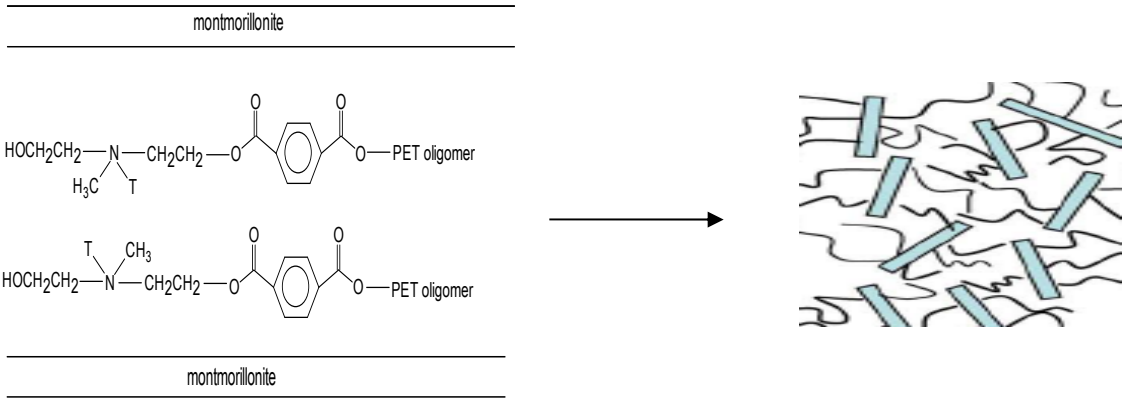

Figure 10: Intercalation of PET molecules into clay gallery.

The nanocomposite morphology can be investigated by AFM studies. The stiff (crystalline) regions usually appear in lighter colors in the height, whereas the darker places correspond to softer areas (amorphous domains), which are darker in the lateral force scan.

Crystallite sizes (star like bright zone) in the MMT-filled nanocomposite, which has layered morphology resulting from MMT plates (Figure 11B), have become smaller than unfilled regular PET with non-layered morphology as shown in Figure 11A. AFM is the most suitable technique for reflecting the true shapes of the exfoliated particles of MMTs on the

film surface of the PETMMT nanocomposite samples [22].

In the previous study, it was found that the molecular conformation in the crystalline PET is totally trans [31]. Hence the crystal zone has no free space. In this study, as shown in Figure 15, MMT layers are not capable of penetration into crystal zone and are distributed in the amorphous free volume. Thus they are not uniformly distributed in all directions throughout the structure (Figure 12).

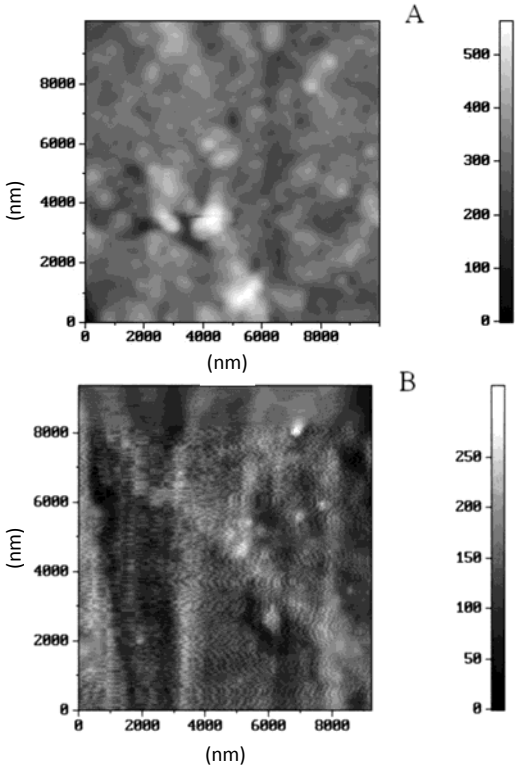

Figure 11: AFM morphology of (A) pure PET and (B) PET nanocomposite with 3 %wt organoclay.

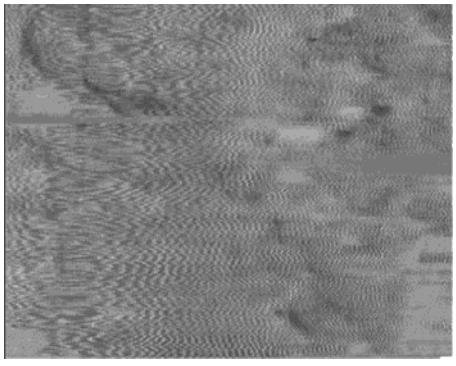

Figure 12: AFM morphology of PET nanocomposite with 3 %wt organoclay incorporated from amorphous zone in free space; AFM images of bulk are obtained in contact mode.

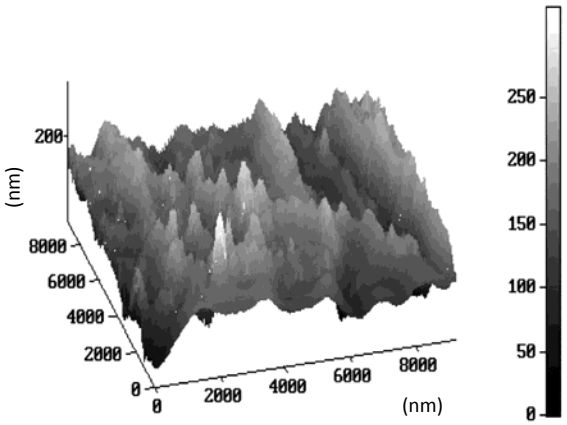

Figure 13: The broken mirror like lamellae AFM morphology of PET nanocomposite (with the system operating in tapping mode).

The gas barrier properties are especially enhanced by the increase in tortuosity affected by structural factors. These properties are dependent on the spacing between the nanoplatelets and clay platelet orientation [32]. Conventionally, the only way to achieve decreased spacing between the platelets, and thereby increasing tortuosity and decreasing permeability, is increasing the overall clay content of the nanocomposite (Table 5).

Table 5: The gas barrier properties of pure PET and nanocomposite.

PET Nano composite (2×50×50 mm)	MMT Closite 30B %wt	O_2 Pressure drop (ΔP) (P_0= 15 atm; t = 30 days)
Pure PET	-	0.8 atm
Nano PET2	2	0.6 atm
Nano PET3	3	0.4 atm
Nano PET5	5	0.7 atm

CONCLUSIONS

The stain products were removed with decreasing reaction time and temperature by the implementation of combination methods between melt polycondensation process and SSP. Disappearing XRD spectrum in 2°-5°2θ

regions of the nanocomposite indicates the exfoliated structure of layered silicates in polymer matrix. A three dimensional AFM image of the PET nanocomposite, operated in tapping mode, shows a broken mirror like lamella structure. Moreover, increasing organo-MMT amount broadens the XRD spectrum of the PET nanocomposite in 10°-30°2θ region, showing that the triclinic crystals are getting smaller. The higher the amount of organo-MMT is, the smaller the crystal size becomes.

DSC results indicate an increased crystallization rate but a smaller crystal size (the reduction of ΔT) in accordance with the increased organo-MMT amount. Increasing organo-MMT amount increases the HDT, tensile modulus, and tensile strength of the PET nanocomposite. PET nanocomposite with 3 %wt organo-MMT leads to an about 50% reduction in O_2 pressure drop (or relative oxygen permeability) compared with a homo structure. However, increasing organo-MMT amount shows fluctuations in the relative oxygen pressure drop.

NOMENCLATURE

AFM : Atomic Force Microscopy

DSC : Differential Scanning Calorimetry

MMT : Montmorillonite

PET : Polyethylene Terephthalate

SSP : Solid State Polymerization

XRD : X-Ray Diffraction

ΔH_c : Enthalpy Crystal Formation

$t_{1/2}$: Time (hr)

$T_{c,on}$: On set temperature (°C)

T_c : Temperature (°C)

X : Cooling rate (°C/min)

REFERENCES

[1] Ray S. S. and Okamoto M., "Polymer/Layered Silicate Nanocomposites: A Review from Preparation to Processing," *Progress in Polymer Science*, **2003**, *28*, 1539-1641.

[2] Gupta B., Lacrampe M-F., Krawczak P., "Polyamide-6/ Clay Nanocomposites, A Critical Review," *Polymer and Polymer Composites*, **2006**, *14*, 13-38.

[3] Lee W. D. and. Im S. S, "Dispersibility of Clay and Crystallization Kinetics for *In Situ* Polymerized PET/Pristine and Modified Montmorillonite Nanocomposites," *Journal of Polymer Science Part B: Polymer Physics,* **2007**, *28*, 45-53.

[4] Hwang S. Y., Lee W. D., Lim J. S., Park K. H, et al., "Dispersibility of Clay and Crystallization Kinetics for *In Situ* Polymerized PET/Pristine and Modified Montmorillonite Nanocomposites, " *Journal of Polymer Science Part B: Polymer Physics*, **2008**, *46*, 1022-1035.

[5] Mainar K. K., "Polymeric Nanocomposites a Review," *Polymer-Plastics Technology and Engineering*, **2004**, *43*, 427-443.

[6] Chang J.H., Kim S. J., Joo Yong L., and Im S., "Poly Ethylene Terephthalate Nanocomposites by in Situ Interlayer Polymerization," *Polymer,* **2004**, *45,* 919-926.

[7] Ke Y., Long Ch., and Qi Z., "Crystallization, Properties, and Crystal and Nanoscale Morphology of PET-Clay Nanocomposites," *Journal of Applied Polymer Science*, **1999**, *71*, 1139-1146.

[8] Costache M. C., Heidecker M. J., Manias E., and Wilkie Ch. A., "Preparation and Characterization of Poly (Ethylene Terephthalate)/Clay Nanocomposites by Melt Blending Using Thermally Stable Surfactants," *Polymers for Advanced Technologies*, **2006**, *17*, 764–771.

[9] Pavlidoua S. and Papaspyrides C. D., "A Review on Polymer Layered Silicate Nanocomposites," *Progress in Polymer Science,* **2008**, *33*, 1119-1198.

[10] Esmailzadeh A., et al, "Mechanical and Crystallization Analyses of Layered Silicate Polyethylene Terephthalate Nanocomposites," Prepared by in Situ Polymerization *Asia/Australia Regional Meeting,* Kish island, Iran, **2011**, 15-17.

[11] Ou C.F., Ho M.T., and Lin J.R., "Synthesis and Characterization of Poly (Ethylene Terephthalate) Nanocomposites with

Organoclay," *Journal of Applied Polymer Science*, **2004**, *91*, 140-145.

[12] Patro T. U., Khakhar D. V., and Misra A., "Phosphonium-Based Layered Silicate—Poly (Ethylene Terephthalate) Nanocomposites: Stability, Thermal and Mechanical Properties," *Journal of Applied Polymer Science*, **2009**, *113*, 1720-1732.

[13] Chang J. H., Mun M. K., Lee C., "Poly (Ethylene Terephthalate) Nanocomposite Fibers by in Situ Polymerization: The Thermomechanical Properties and Morphology," *Journal of Applied Polymer Science*, **2005**, *98*, 2009-2016.

[14] Guan G. H., Li C. C., and Zhang D., "Spinning and Properties of Poly (Ethylene Terephthalate)/Organomontmorillonite Nanocomposite Fibers," *Journal of Applied Polymer Science*, **2005**, *95*, 1443-1447.

[15] Guan G., Li C., Zhang D., and Jin Y., "The Effects of Metallic Derivatives Released from Montmorillonite on the Thermal Stability of Poly(EthyleneTerephthalate)/Montmorillonite Nanocomposites," *Journal of Applied Polymer Science*, **2006**, *101*, 1692-1699.

[16] Jabarin S. A., "Polymeric Materials Encyclopedia," **1996**, *8*, CRC press, 6078-6085, 6091-6100.

[17] Wiesendanger R., "Scanning Probe Microscopy and Spectroscopy," **1994** (Cambridge: Cambridge University Press).

[18] Calcagno C. I. W., Mariani C. M., Teixeira S. R., and Mauler R. S., "The Effect of Organic Modifier of the Clay on the Morphology and Crystallization Properties of PET Nanocomposites," *Polymer*, **2007**, *48*, 966-974.

[19] Sharma R., Joshi H., and Jain P., "Short Review on the Crystallization Behavior of PET/Clay Nanocomposites," *Journal of Chemical Engineering and Materials Science*, **2011**, *2*, 39-43.

[20] Kim T. Y., Lofgren E. A., and Jabarin S. A., "Solid-State Polymerization of Poly (Ethylene Terephthalate). I. Experimental Study of the Reaction Kinetics and Properties," *Journal of Applied polymer Science*, **2003**, *89*, 197-212.

[21] Neef C. J. and Ferraris J. P., "Improved Synthetic Procedure and Molecular Weight Control," *Macromolecules*, **2000**, *33*, 2311–2314.

[22] Dini M., Carreau P. J., Kamal M.R., Minh-Tan, et al., "Effect Of Organoclay Content In Solid-State Polymerization Of Poly (Ethylene Terephthalate)," *Society of Plastics Engineers* (SPE) **2014**,10,2417

[23] Dini M., Carreau P. J., Kamal M. R., Ton-That M. T., et al., "Solid-State Polymerization of Poly (Ethylene Terephthalate): Effect of Organoclay Concentration," *Polymer Engineering Science*, **2014**, First published online: 22 January. doi:10.1002/pen.23853.

[24] Chacko A., Sadiku E. R., and Vorster O. C., "The Rheological and Mechanical Properties of Organoclay Nanocomposites," *Journal of Reinforced Plastics and Composites*, **2010**, *29*, 4.

[25] Guihe L., Zhifeng F., and Ding C., "Study on the Synthesis and Properties of PET Using Hydrotalcite as Catalyst," *China Petroleum Processing and Petrochemical Technology*, **2013**, 15, 65-69

[26] Ke Y. C. and Stroeve P., "Polymer-Layered Silicate and Silica Nanocomposites," Radarweg 29 P. O. Box 211, 1000 AE Amsterdam, the Netherlands Elsevier B. V. ISBN: 0-444-51570-4 (1St ed.) **2005** P224, 322.

[27] Wang Y., Gao J., Ma Y., and Agarwal U. S., "Study on mechanical properties, thermal stability and crystallization behavior of PET/MMT nanocomposites," Composites: Part B 37 **2006**, 399.

[28] Yelkovan S., Yılmaz D., and Aksoy K., "A study of organo-modified clay type on pet-clay based nanocomposite properties," *Usak University Journal of Material Sciences,* **2014**, *1*, 33 –46.

[29] Hegde R. R., Bhat G. S., and Deshpande B., "Crystallization Kinetics and Morphology of Melt Spun Poly (Ethylene Terephthalate) Nanocomposite Fibers," *Express Polymer Letters*, **2013**, 7, 821–831.

[30] Bushroa A. R., Rahbari b R. G., Masjuki d H. H., and Muhamadc M. R., "Approximation of Crystallite Size and Microstrain Via XRD Line Broadening Analysis," Vacuum 86, **2012**, 1107-1112

[31] Avolio R., Gentile G., Avella M., Carfagna C., et al. "Polymer–filler interactions in PET/CaCO3 nanocomposites: Chain ordering at the interface and physical properties," *European Polymer Journal* **2013**, *49*, 419-427.

[32] Carrera M. C., Erdmann E., and H. A. "Destéfanis Barrier Properties and Structural Study of